Short Communication

Study on Electrodeposition of ZnNi/Al₂O₃ Composite Coating on 40Mn Steel and its Corrosion Behavior in Simulated Concrete Pore Solution

Yingguang Wang[1,], Yali Qi[2]*

[1] College of Architectural Engineering, Jilin Province Economic Management Cadre College, China Jilin, Changchun 130000
[2] College of Architectural Engineering, Jilin Engineering Vocational College, China Jilin, Siping 136001
[*]E-mail: wyg_college@yeah.net

Abstract: The ZnNi/Al₂O₃ composite coating is electrodeposited on 40Mn steel as construction material and passivation treatment is used to greatly improve its corrosion resistance in simulated concrete pore solution. It is found out that the Al₂O₃ nano-particle in the plating solution will increase the mass transfer rate of zinc ions and nickel ions that results in the increase of thickness. The addition of Al₂O₃ nano-particles is beneficial to refine grain size that results in the decrease of roughness and increase of wear resistance. The corrosion resistance of ZnNi/Al₂O₃ composite coating is better than that of ZnNi coating due to the doped non-conductive Al₂O₃ nano-particles. The corrosion current density of ZnNi/Al₂O₃ composite coating is decreased extremely after passivation treatment due to the formation of $Zn(OH)_2$ and Cr_2O_3 resulting in the great increase of corrosion resistance.

1. INTRODUCTION

As one of the most commonly used materials in the field of industry and construction fields, the corrosion resistance of carbon steel has attracted more and more attentions [1-5]. However, carbon steels are easily corroded in air, especially in hot and humid environment. In order to protect and improve the corrosion resistance of carbon steel, it is usually required to prepare zinc, copper, chromium and alloy coatings on the surface of carbon steel [6-10]. It is found that plating zinc on the surface of carbon steel to improve corrosion resistance accounts for about 60% of the total electroplating. But with the development of modern construction, the quality requirements of the

protective coating for carbon steel are becoming higher and higher. The traditional zinc layer cannot greatly improve the corrosion resistance of carbon steel in the harsh construction environment, such as concrete pore solution. Therefore, some alloys such as ZnNi, ZnFe, ZnCo, NiW, NiFe, etc are reported that have better corrosion resistance than traditional zinc coating [11-16]. Among them, Zn-Ni alloy coating has attracted more attentions because of its advantages of high corrosion resistance, excellent bonding force and simple process parameter. Electrodeposition is an effective and efficient method to fabricate ZnNi alloy coating on carbon steel due to its lower cost and higher stability. Many scholars prepare ZnNi alloys with better properties by electrodepostion. It is found out that the corrosion resistance of ZnNi alloy coating is 4~10 times higher than that of zinc plating.

With the development of nano-technology, it is reported that doping nano-particles during ZnNi electrodeposition to prepare the composite coating can extremely improve its corrosion resistance, so as to effectively protect the carbon steel substrate. By using the excellent properties of nano-materials and metal co-deposition, the composite coatings possess much higher hardness, better wear resistance and optimal corrosion resistance. Alumina is commonly known as corundum which has stable chemical properties with strong hardness and excellent corrosion resistance [17-20]. In this paper, $ZnNi/Al_2O_3$ composite coating is prepared by combining nano-alumina particles and the superior performance of ZnNi alloy through electrodeposition technology. Finally, the $ZnNi/Al_2O_3$ composite coating is passivated from solution containing trivalent chromium which greatly improves its corrosion resistance. It is of great significance and innovative to further broaden the application fields of ZnNi alloy coatings on the carbon steel as construction material.

2. EXPERIMENTAL

2.1 Plating solution and parameters

As a typical carbon steel, 40Mn steel plate is used as the substrate in the plating process with surface area of 2 cm×3 cm. The substrate is polished firstly. And then, 30 g/L NaOH solution is used to get rid of oil on the surface of substrate. After the substrate is cleaned, the 15% HCl solution is chosen to remove the rust on the substrate surface. The pure nickel plate with surface area of 3 cm×5 cm is utilized as the counter electrode. The detailed chemical composition of plating solution (100 mL) is as follows: 100 g/L $ZnCl_2$, 50 g/L $NiCl_2$, 120 g/L KCl, 30 g/L NH_4Cl, 35 g/L H_3BO_3 and 10 g/L Al_2O_3 nano-particles. Before Al_2O_3 nano-particles are added into the electroplating solution, the solution of Al_2O_3 nano-particle is stirred for 6 hours and then ultrasonic is applied for 15 minutes to reduce the agglomeration effect. The current density is 2.5 A/dm^2 for 1 hour at the temperature of 60 °C and pH=6 with continuous mechanical agitation.

2.2 Passivation treatment

After the electrodeposition of $NiZn/Al_2O_3$ composite coating on 40Mn steel substrate is finished, the passivation treatment is needed. The chemical composition of passivation solution is as

follows: 40 g/L $Cr(NO_3)_3$, 10 g/L $NaNO_3$, 10 g/L $H_2C_2O_4$ and 15 g/L $C_3H_4O_4$. The passivation temperature is 50 °C and the passivation time is 15 minutes at pH=3.

2.3 Performance testing

Parstat 2273 electrochemical station is used to test the cyclic voltammetry curves of 40Mn steel in different plating solutions with 0.1 M Zn^{2+}, 0.1 M Ni^{2+}, 0.1 M Zn^{2+}+0.1 M Ni^{2+} and 0.1 M Zn^{2+}+0.1 M Ni^{2+} with 10 g/L Al_2O_3 nano-particle respectively at the 20 mV/s scan rate. The 40 Mn steel plate with surface area of 1 cm×1 cm is as the working electrode and the counter electrode is platinum plate with surface area of 2 cm×2 cm. The reference electrode is the saturated calomel electrode. The Klatencor P7 is used to test the roughness and thickness of ZnNi and ZnNi composite coating. The composition of samples is analyzed by EDX300B. The friction abrasion meter HSR2M is used to test the wear resistance of samples based on the scratch on the surface at the condition of 5 N loading force for 30 minutes. Scan electron microscope TM3030 is chosen to observe the surface morphology at 15 kV. The corrosion resistance of samples in 100 ml simulated concrete pore solution (2 g/L $Ca(OH)_2$ and 3 g/L NaCl) is determined by polarization curves at the scan rate of 1 mV/s. The sample with 1 cm ×1 cm size is as the working electrode while the platinum plate with surface area of 2 cm×2 cm is as the counter electrode. The saturated calomel electrode is as the reference electrode.

3. RESTULS AND DISCUSSIONS

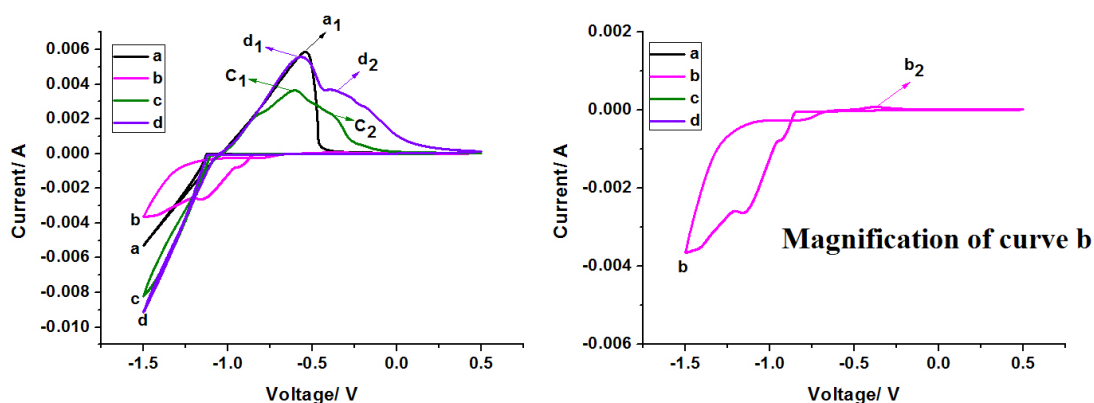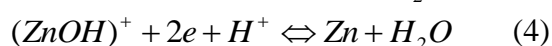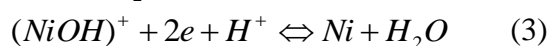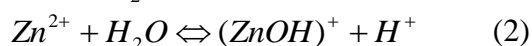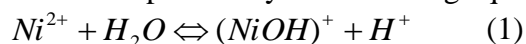*3.1 Cyclic voltammetry curve of 40Mn steel plate in different solutions*

Figure 1. Cyclic voltammetry curves of 40Mn steel plate in different plating solutions; a: 0.1 mol/L $ZnCl_2$; b: 0.1 mol/L $NiCl_2$; c: 0.1 mol/L $ZnCl_2$ and 0.1 mol/L $NiCl_2$; d: 0.1 mol/L $ZnCl_2$, 0.1 mol/L $NiCl_2$ and 10 g/L Al_2O_3 nano-particles;

The cyclic voltammetry curves of 40Mn steel plate in different plating solutions are shown in Figure 1. It can be seen that, four cyclic voltammetry curves of different plating solution are different due to different reduction and oxidation reactions. According to curve a, the cathode current at the

voltage of -1.5 V is about -5.28 mA which represent the reduction of zinc ions. The oxidation peak of zinc can be found at the potential of -0.54 V(a_1). Curve b stands for the reduction and oxidation of nickel. The cathode current is around -3.65 mA at the potential of -1.5 V while the oxidation peak of nickel is around -0.372 (b_2) which is more positive than that of zinc. According to the curve c, the cathode current of solution with both zinc and nickel ions is about -8.11 mA at the potential of -1.5 V. Moreover, two obvious oxidation peaks can be observed at the potential of -0.59 V (c_1) and -0.39 V (c_2) respectively which represents the dissolution of zinc and nickel. The curve d is the cyclic voltammetry of 40 Mn steel plate in the plating solution with nickel ions, zinc ions and Al_2O_3 nano-particle. It is obvious the cathode current is around -9.12 mA at the potential of -1.5 V which indicates that Al_2O_3 nan-particle in the plating solution is beneficial to increase the cathode current and deposition rate. Two oxidation peaks of ZnNi/Al_2O_3 composite alloys are found at the potential of -0.58 V (d_1) and -2.28 V (d_2) that indicates the dissolution of zinc and nickel. The intensity of oxidation peaks of ZnNi/Al_2O_3 composite alloys are higher than ZnNi alloys, which means that more zinc and nickel are electrodeposited on the 40Mn steel due to the introduction of Al_2O_3 nano-particle. The co-deposition of ZnNi can be explained by the following equations below [21-23].

$$Ni^{2+} + H_2O \Leftrightarrow (NiOH)^+ + H^+ \qquad (1)$$
$$Zn^{2+} + H_2O \Leftrightarrow (ZnOH)^+ + H^+ \qquad (2)$$
$$(NiOH)^+ + 2e + H^+ \Leftrightarrow Ni + H_2O \qquad (3)$$
$$(ZnOH)^+ + 2e + H^+ \Leftrightarrow Zn + H_2O \qquad (4)$$

As the electrodeposition proceeds, the pH value near the cathode increases to form $(NiOH)^+$ and $Zn(OH)^+$ which are easy to get electrons to be reduced to the corresponding metal. In addition, some zinc ions and nickel ions are directly reduced on the surface of Al_2O_3 nano-particles to form ZnNi/Al_2O_3 composite alloy with alumina particles wrapped in the alloy.

3.2 Roughness and thickness of ZnNi/Al₂O₃ composite coating

The surface profile between the substrate and the coating is observed by surface profiler and the average step height is calculated to be defined as the thickness of the samples shown in Figure 2 and Table 2. It can be seen that the thickness of ZnNi coating electrodeposited from the solution without Al_2O_3 nano-particle is approximate 21.39 μm. When 10 g/L Al_2O_3 nano-particle is added into the plating solution, the thickness of electrodeposited ZnNi/Al_2O_3 composite coating is increased to 26.42 μm. From the previous analysis of cyclic voltammetry, the addition of nano-alumina particles into the plating solution is beneficial to increase the cathode reaction current and deposition rate. On the one hand, the surface of Al_2O_3 nano-particle can absorb nickel ions and zinc ions, which accelerate the mass transfer rate of metal ions. On the other hand, under the action of electric field and diffusion, Al_2O_3 nano-particle is adsorbed on the cathode surface. The zinc ions and nickel ions are directly reduced to form ZnNi alloy on the surface of nano-alumina particles. At the same time, the Al_2O_3 nano-particles are wrapped in the alloy coating, forming a composite coating and increasing the reaction current. Moreover, after the passivation treatment, the thicknesss of ZnNi/Al_2O_3 composite

coating does not change much. It shows that passivation treatment has little effect on the thickness of composite coating.
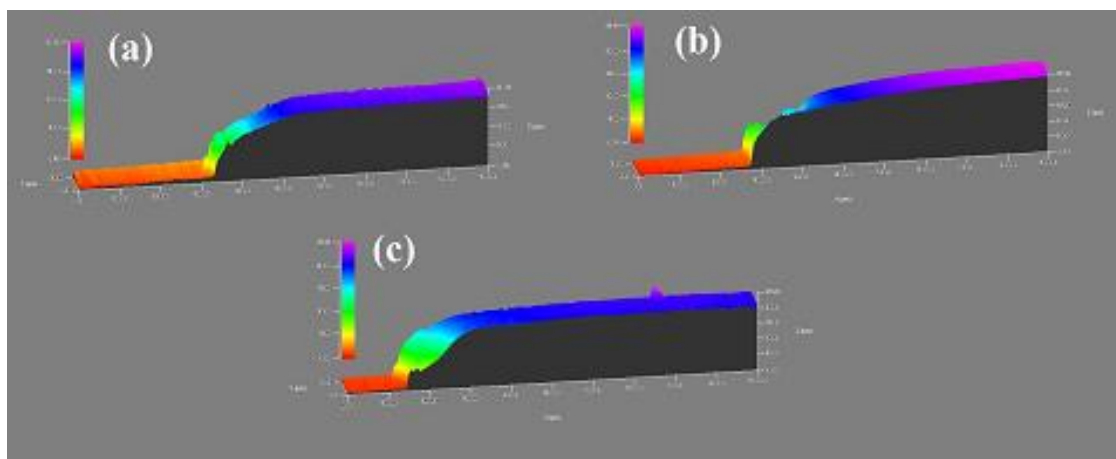

Figure 2. Surface profile of ZnNi coating and ZnNi/Al$_2$O$_3$ composite coating; a. ZnNi coating; b. ZnNi/Al$_2$O$_3$ composite coating; c. ZnNi/Al$_2$O$_3$ composite coating after passivation treatment;

Table 1. Thickness of ZnNi coating and ZnNi/Al$_2$O$_3$ composite coating; a. ZnNi coating; b. ZnNi/Al$_2$O$_3$ composite coating; c. ZnNi/Al$_2$O$_3$ composite coating after passivation treatment;

Sample	Minimum thickness(μm)	Maximum thickness(μm)	Average thickness(μm)
a	17.24	22.84	21.39
b	19.43	28.39	26.42
c	20.12	28.72	26.92
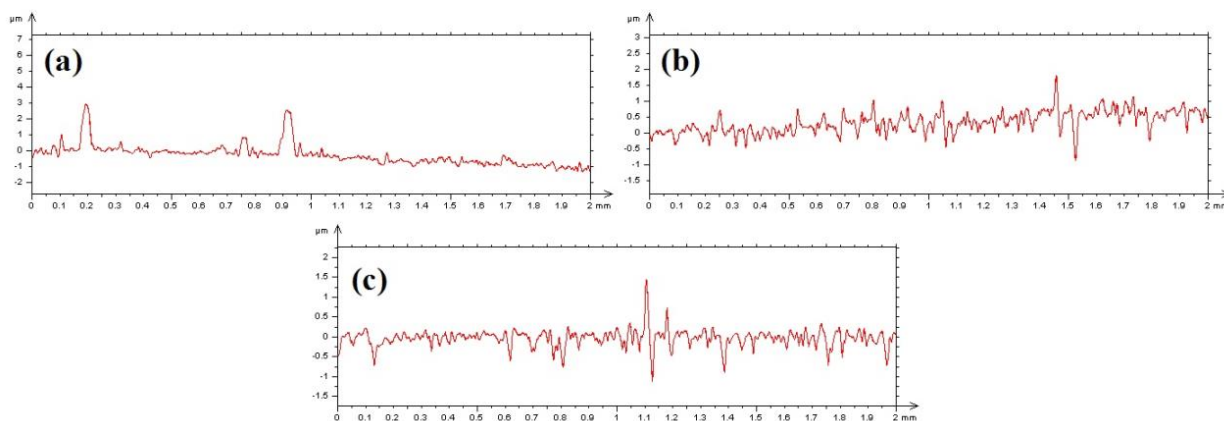
Figure 3. Surface waviness of ZnNi coating and ZnNi/Al$_2$O$_3$ composite coating; a. ZnNi coating; b. ZnNi/Al$_2$O$_3$ composite coating; c. ZnNi/Al$_2$O$_3$ composite coating after passivation treatment;

Figure 4. Surface roughness of ZnNi coating and ZnNi/Al$_2$O$_3$ composite coating; a. ZnNi coating; b. ZnNi/Al$_2$O$_3$ composite coating; c. ZnNi/Al$_2$O$_3$ composite coating after passivation treatment;

Table 2. Roughness of ZnNi coating and ZnNi/Al$_2$O$_3$ composite coating; a. ZnNi coating; b. ZnNi/Al$_2$O$_3$ composite coating; c. ZnNi/Al$_2$O$_3$ composite coating after passivation treatment;
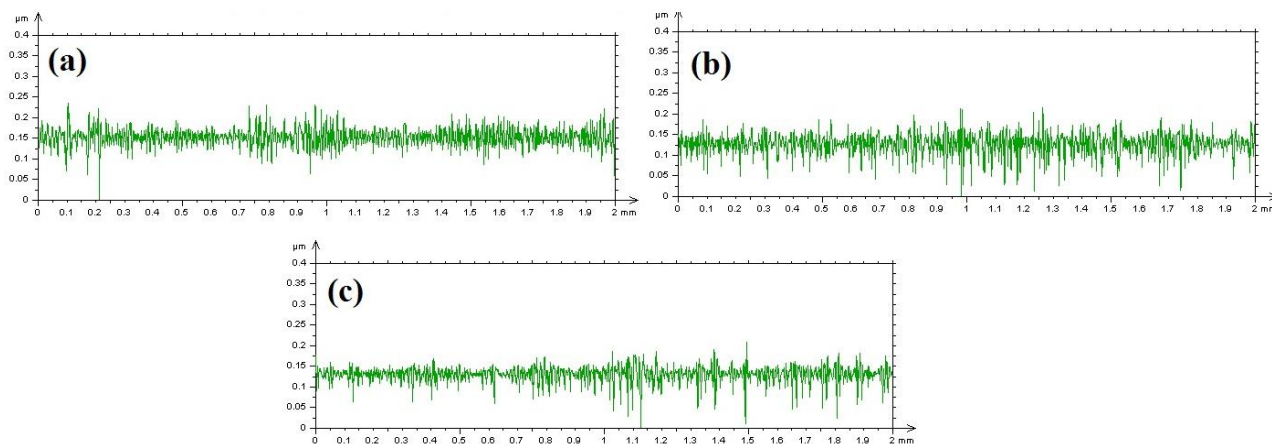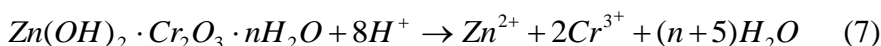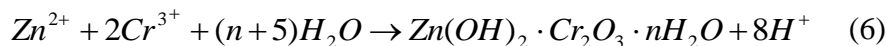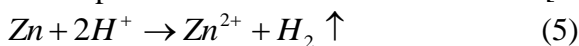
Sample	Ra(μm)
a	0.314
b	0.152
c	0.136

Surface roughness refers to the unevenness of material surface. The smaller the sample surface roughness is, the smoother the surface will be. The surface roughness of the coating is closely related to the hardness, wear resistance, corrosion resistance and morphology [24-25]. In this paper, the contour arithmetic mean deviation R_a is used to calculate the surface roughness of the coating. A profilometer is used to get the waviness of the coating surface firstly, and then a fitting tool is used to calculate R_a based on the waviness curve. The result is shown in Figure 3, Figure 4 and Table 2. The surface roughness of ZnNi electrodeposited coating is equal to 0.314 μm while the surface roughness of ZnNi/Al$_2$O$_3$ composite coating is around 0.152 μm which is only half of that of ZnNi electrodeposited coating. The roughness of ZnNi/Al$_2$O$_3$ composite coating after passivation treatment is the smallest, which is equal to 0.136 μm. The Zn(OH)$_2$ and Cr$_2$O$_3$ formed during the passivation treatment cover the coating surface, so as to decrease the roughness.

3.3 Composition and surface morphology of ZnNi/Al$_2$O$_3$ composite coating

The chemical composition of ZnNi coating and ZnNi/Al$_2$O$_3$ composite coating is listed in Table 3. Form the data of Table 3, it is obvious that the ZnNi electrodeposited coating is composed of 14.3% Ni and 85.7% Zn. The zinc content is higher than nickel content due to the anomalous co-deposition. The element Al is found in the ZnNi/Al$_2$O$_3$ composite coating which verifies that Al$_2$O$_3$

nano-particle is successfully doped into the ZnNi coating. Moreover, the nickel content in the ZnNi/Al$_2$O$_3$ composite coating is higher than that of in the ZnNi coating. It indicates that the Al$_2$O$_3$ in the plating solution will improve the electrodeposition of nickel. The adsorption of nickel ions on alumina particles is stronger than that on zinc ions, so when alumina migrates to the cathode surface under the action of electric field and diffusion, the mass transfer rate of nickel ions can be accelerated, so as to improve the nickel content in the coating. After the passivation treatment, the amount of nickel and zinc in the ZnNi/Al$_2$O$_3$ composite coating decrease simultaneously and the chromium is detected. The mechanism of passivation treatment is as follows [26]:

$$Zn + 2H^+ \rightarrow Zn^{2+} + H_2 \uparrow \qquad (5)$$

$$Zn^{2+} + 2Cr^{3+} + (n+5)H_2O \rightarrow Zn(OH)_2 \cdot Cr_2O_3 \cdot nH_2O + 8H^+ \qquad (6)$$

$$Zn(OH)_2 \cdot Cr_2O_3 \cdot nH_2O + 8H^+ \rightarrow Zn^{2+} + 2Cr^{3+} + (n+5)H_2O \qquad (7)$$

Zinc is oxidized to zinc ions, which increases the pH value near the ZnNi alloy surface. Zinc hydroxide and chromium oxide are formed under alkaline conditions, which are the main components of passivation coating. However, in an acidic environment, the generated passivation coating will be dissolved. The passivation coating formation is a dynamic equilibrium process. Many similar passivation films are prepared on the surface of ZnNi alloys. For example, Muller et al. prepares black passivated ZnNi alloys from solutions containing Cr^{6+} ions which possess higher nickel content and small amount of molybdenum [27]. However, the hexavalent chromium is harmful and toxic. Moreover, Foster et al. investigates the trivalent chromium passivation film on ZnNi alloys [28]. The prepared passivation film is composed of 11% chromium which is similar to the result in the paper. Kozaderov et al. also study the trivalent chromium passivation of ZnNi alloys. They find that the simonkolleite Zn$_5$(OH)$_8$Cl$_2$·H$_2$O formed during the passivation can greatly improve the corrosion resistance [29]. The difference between trivalent chromium passivation and hexavalent chromium passivation is researched by Zaki published in the journal of metal finish [30].

Table 3. Chemical composition of ZnNi coating and ZnNi/Al$_2$O$_3$ composite coating; a. ZnNi coating; b. ZnNi/Al$_2$O$_3$ composite coating; c. ZnNi/Al$_2$O$_3$ composite coating after passivation treatment;

Samples	Ni(%)	Zn(%)	Al(%)	Cr(%)
a	14.3	85.7	-	-
b	28.2	64.6	7.2	-
c	24.1	60.2	6.5	9.2

Figure 5 shows the surface morphology of ZnNi coating and ZnNi/Al$_2$O$_3$ composite coating. According to the Figure 5, the ZnNi coating and ZnNi/Al$_2$O$_3$ composite coating both show granular structure. Compared with ZnNi coating, the ZnNi/Al$_2$O$_3$ composite coating has denser and smaller granular structure. In the process of composite electrodeposition, the addition of Al$_2$O$_3$ nano-particles is beneficial to the formation of new crystal nuclei, and can inhibit the aggregation and growth of grain, which plays a role in refining metal grain. Some dark products can be found and covered on the

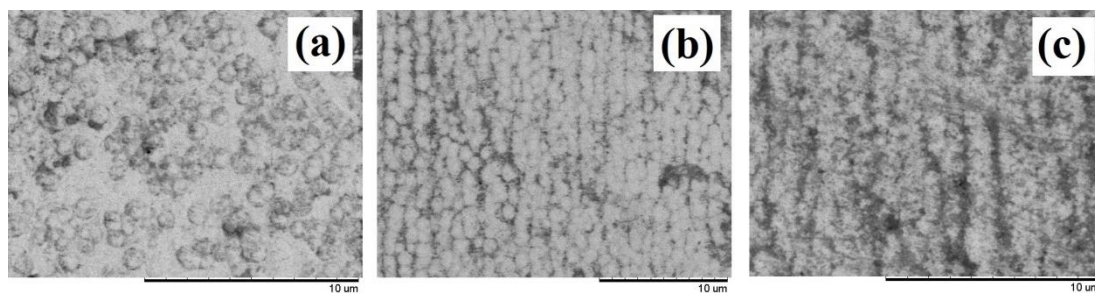surface of composite coating after passivation treatment which is the zinc hydroxide and chromium oxide.

Figure 5. Surface morphology of ZnNi coating and ZnNi/Al$_2$O$_3$ composite coating; a. ZnNi coating; b. ZnNi/Al$_2$O$_3$ composite coating; c. ZnNi/Al$_2$O$_3$ composite coating after passivation treatment;
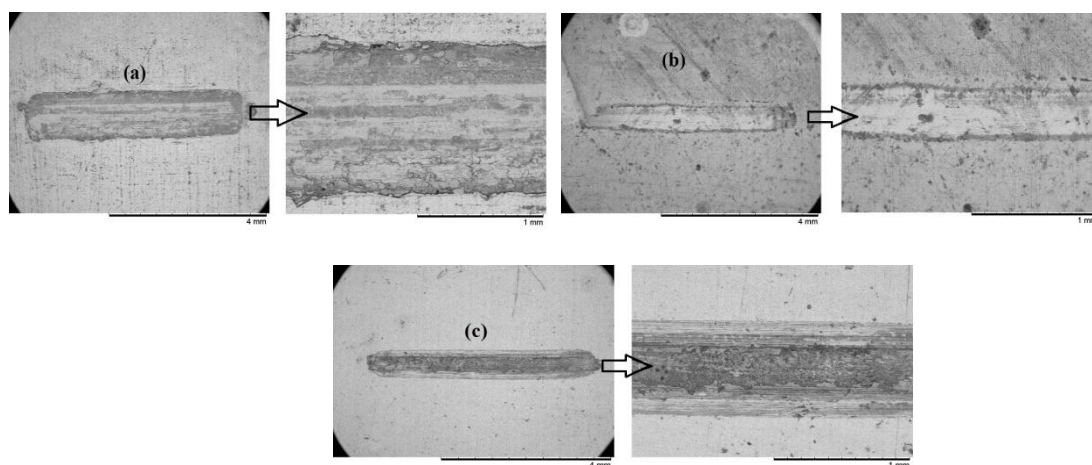

Figure 6. Scratch morphology on the surface of ZnNi coating and ZnNi/Al$_2$O$_3$ composite coating; a. ZnNi coating; b. ZnNi/Al$_2$O$_3$ composite coating; c. ZnNi/Al$_2$O$_3$ composite coating after passivation treatment; The loading force is 5 N for 30 minutes.

The friction abrasion meter HSR2M is used to test the wear resistance of samples based on the scratch on the surface at the condition of 5 N loading force for 30 minutes shown in Figure 5. The scratch on the surface of ZnNi coating is larger than ZnNi/Al$_2$O$_3$, which indicates that the wear resistance of ZnNi/Al$_2$O$_3$ composite coating is better than ZnNi coating. Alumina has high hardness, from the previous analysis, alumina embedded in ZnNi alloy is conducive to refining the surface particles of the coating and greatly improving the wear resistance. However, after passivation treatment, the size of scratch on the ZnNi/Al$_2$O$_3$composite coating has little change.

3.4 Corrosion resistance of ZnNi/Al$_2$O$_3$ composite coating

According to the Figure 7 and Table 4, the corrosion current density and corrosion potential of substrate is -1.026 V and 57.54×10^{-6} A/cm^2 respectively that indicates poor corrosion resistance.

Compared with the substrate, the corrosion resistance of ZnNi coating is better, which possesses -0.973 V corrosion potential and 10.23×10^{-6} A/cm^2 corrosion current density. According to some researches, the main corrosion products of ZnNi coating during corrosion process are zinc chloride, zinc hydroxide and nickel oxide [31]. The corrosion current density of ZnNi/Al$_2$O$_3$ composite coating is 5.49×10^{-6} A/cm^2 which is smaller than that of ZnNi coating. At the initial stage of corrosion, a large number of Al$_2$O$_3$ nano-particles bind closely to the ZnNi grains in the coating. The Al$_2$O$_3$ nano-particles separate the corrosive medium from the grain, effectively reducing the corrosion of the composite coating in the solution. Moreover, the Al$_2$O$_3$ nano-particle is not conductive, which will disperse current during corrosion and inhibit the corrosion of the composite coating. However, the corrosion current density of ZnNi/Al$_2$O$_3$ composite coating is decreased extremely after passivation treatment due to the formation of Zn(OH)$_2$ and Cr$_2$O$_3$ resulting in the great increase of corrosion resistance.
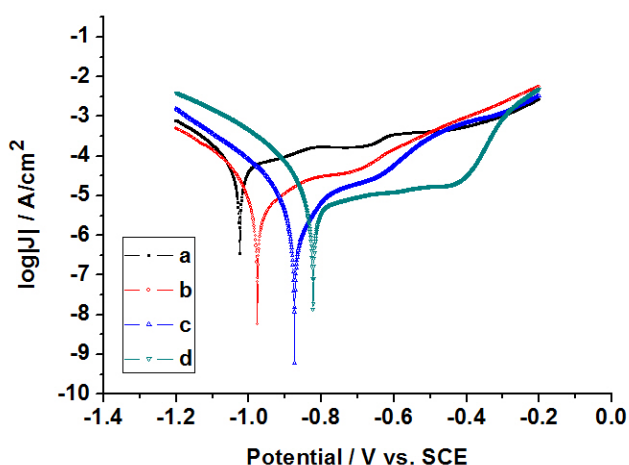

Figure 7. Polarization curves of ZnNi coating and ZnNi composite coating in simulated concrete pore solution; a. 40Mn steel; b. ZnNi coating; c. ZnNi/Al$_2$O$_3$ composite coating; d. ZnNi/Al$_2$O$_3$ composite coating after passivation treatment;

Table 4. E_{corr} and J_{corr} of different samples in simulated concrete pore solution

Samples	E_{corr}(V)	J_{corr}(A/cm^2)
a	-1.026	57.54×10^{-6}
b	-0.973	10.23×10^{-6}
c	-0.876	5.49×10^{-6}
d	-0.827	3.63×10^{-6}

4. CONCLUSIONS

The ZnNi/Al$_2$O$_3$ composite coating is electrodeposited on the surface of 40Mn steel. The surface morphology, roughness, thickness, wear resistance, corrosion resistance of ZnNi coating and ZnNi/Al$_2$O$_3$ composite coating are compared and investigated. ZnNi electrodeposition is an anomalous

co-deposition. The zinc ions and nickel ions are directly reduced on the surface of Al_2O_3 nano-particles to form $ZnNi/Al_2O_3$ composite alloy with alumina particles doped in the alloy.

(1) The Al_2O_3 nano-particle in the plating solution is beneficial to increase the mass transfer rate of nickel and zinc ions, so as to increase the deposition rate and thickness. The surface roughness of ZnNi electrodeposited coating is equal to 0.314 μm while the surface roughness of $ZnNi/Al_2O_3$ composite coating is around 0.152 μm. The roughness of $ZnNi/Al_2O_3$ composite coating after passivation treatment is the smallest, which is equal to 0.136 μm.

(2) The Al_2O_3 nano-particle in the plating solution will improve the electrodeposition of nickel, so as to improve the nickel content in the coating. After the passivation treatment, the amount of nickel and zinc in the $ZnNi/Al_2O_3$ composite coating decrease simultaneously and the chromium is detected. Compared with ZnNi coating, the $ZnNi/Al_2O_3$ composite coating has denser and smaller granular structure that results in better wear resistance. The corrosion current density of $ZnNi/Al_2O_3$ composite coating is $5.49×10^{-6}$ A/cm^2 which is smaller than that of ZnNi coating. The corrosion resistance of $ZnNi/Al_2O_3$ composite after passivation treatment is the best.

References

1. Y. Q. Liu and J. J. Shi, *Corros. Sci.*, 205 (2022) 110451.
2. X. Y. Wang, J. B. Zou, J. H. Lin and X. S. Du, *Diamond Relat. Mater*., 120 (2021) 108714.
3. H. Wei, Y. L. Chen, W. Yu, L. Su, X. Wang and D. Tang, *Constr. Build. Mater.*, 239 (2020) 117815.
4. W. J. Guo, A. Umar, Q. Zhao, M. A. Alsaiari, Y. A. Hadeethi, L. Y. Wang and M. S. Pei, *J. Mol. Liq.*, 320 (2020) 114295.
5. A. Thoume, A. Elmakssoudi, D. B. Left, N. Benzbiria, F. Benhiba, M. Dakir, M. Zahouily, A. Zarrouk, M. Azzi and M. Zertoubi, *Chem. Data Collect.*, 30 (2020) 100586.
6. Y. D. Yu, G. Y. Wei, J. W. Lou, H. L. Ge, L. X. Sun and L. Z. Zhu, *Surf. Eng.,* 29 (2013) 234.
7. B. Zhang, H. T. Feng, F. Lin, Y. B. Wang, L. P. Wang, Y. P. Dong and W. Li, *Appl. Surf. Sci*., 378 (2016) 388.
8. X. L. Wang, X. Ye, L. Zhang, Y. Shao, X. X. Zhou, M M. Lu, C. L. Chu, F. Xue and J. Bai, *Surf. Coat. Technol.*, 439 (2022) 128428.
9. A. P. Meshram, A. Gupta and C. Srivastava, *Materials*, 22 (2022) 101413.
10. J. C. Pereira, L. P. M. D. Santos, A. A. C. Alcanfor, H. B. D. Santana, F. X. Feitosa, O. S. Campos, A. N. Correia, P. N. S. Casciano and P. D. L. Neto, *J. Alloys Compd.,* 886 (2021) 161159.
11. Y. H. Hu, Y. D. Yu, H. L. Ge, G. Y. Wei and L. Jiang, *Int. J. Electochem. Sci.*, 14 (2019) 1649.
12. B. Abedini, N. P. Ahmadi, S. Yazdani and L. Magagnin, *Surf. Coat. Technol.*, 372 (2019) 260.
13. O. Hammami, L. Dhouibi and E. Triki, *Surf. Coat, Technol.*, 203 (2009) 2863.
14. B. S. Li, W. W. Zhang, D. D. Li and J. J. Wang, *Mater. Chem. Phys*., 229 (2019) 495.
15. M .Y. Wang, Z. Wang and Z. C. Guo, *Mater. Chem. Phys.*, 148 (2014) 245.
16. J. Zhou, X. H. Meng, P. Ouyang, R. Zhang, H. Y. Liu, C. M. Xu and Z. C. Liu, *J. Electroanal. Chem.*, 919 (2022) 116516.
17. K. Yahiaoui, S. M. Aberkane and A. Naitbouda, *Mater. Chem. Phys.*, 259 (2021) 124045.
18. P. Shanmugaselvam, J. N. R. Yogaraj, S. Sivaraj and N. Jayakrishnan, *Mater. Today:. Proc.,* 37 (2021) 844.
19. X. T. Chang, X. Q. Chen, Q. Y. Zhang, Y. H. Lei, D. S. Wang, J. Y. Li and S. B. Sun, *Corros. Commun.*, 4 (2021) 1.
20. S. Khalilpourazary and J. Salehi, *J. Manuf. Processes*, 39 (2019) 1.
21. P. C. Tulio, S. E. B. Rodrigues and I. A. Carlos, *Surf. Coat. Technol.*, 202 (2007) 91.

22. Z. F. Lodhi, J. M. C. Mol, W. J. Hamer, H. A. Terryn and J. H. W. D. Wit, *Electrochim. Acta*, 52 (2007) 5444.
23. Y. D. Yu, X. X. Zhao, M. G. Li, G. Y. Wei, L. X. Sun and Y. Fu, *Surf. Eng*., 29 (2013) 743.
24. R. Gheisari and A. A. Polycarpou, *Thin Solid Films*, 666 (2018) 66.
25. Q. Z. Xu, Y. Cao, J. Cai, J. F. Yu and C. R. Si, *J. Mater. Res. Technol*., 15 (2021) 384.
26. A. R. E. Sayed, H. M. A. E. Lateef and H. S. Mohran, *Bull. Mater. Sci.,* 38 (2015) 379.
27. C. Muller, M. Sarret and E. Garcia, *Corros. Sci.,* 47 (2005) 307.
28. K. Foster, J. Claypool, W. G. Fahrenholtz, M. O. Keefe, T. Nahlawi and F. Almodovar, *Thin Solid Films*, 735 (2021) 138894.
29. O. Kozaderov, J. Swiatowska, D. Dragoe, D. Burliaev and P. Volovitch, *J. Solid State Electrochem.,* 25 (2021) 1161.
30. N. Zaki, *Met. Finish,* 105 (2007) 425.
31. M. A. E. Hany, R. E. Abdel and S. M. Hossnia, *T. Nonferr. Metal Soc*., 25 (2015) 2807.